Sensors and Materials, Vol. 38, No. 10 (2026) 6183–6194
MYU Tokyo

S & M 4674

Eco-friendly Corn-husk-based Natural-Fiber Composite Panels: Thermal, Acoustic, and Light-induced Degradation Behavior for Sustainable Engineering Applications

Dieter Rahmadiawan,[1,2] Shih-Chen Shi,[1*] Yu Hao,[1] and Guan-Yu Chen[1]

[1]Department of Mechanical Engineering, National Cheng Kung University (NCKU),
No. 1, University Road, Tainan 70101, Taiwan
[2]Department of Mechanical Engineering, Universitas Negeri Padang,
25173 Padang, Sumatera Barat, Indonesia

(Received March 16, 2026; accepted July 27, 2026)

Keywords: corn-husk plywood, thermal insulation, sound absorption, photodegradation, sustainable materials

In this study, we explore the thermal, acoustic, and photodegradation properties of eco-friendly corn-husk plywood of various densities (600, 800, and 1000 kg/m³) and thicknesses (3, 5, and 10 mm). Thermal tests showed that lower density increased internal porosity, reducing thermal conductivity. Acoustic measurements in a small reverberation chamber revealed that sound absorption improved with lower density and greater thickness. The 10-600 (thickness-density) sample achieved a peak absorption coefficient of 0.41 at 6300 Hz and an average coefficient of 0.308, exceeding the 0.200 benchmark for effective sound-absorbing materials. Photodegradation under 28 days of UV-A and visible light exposure led to a 60% decrease in tensile strength and 8.2% weight loss. X-ray photoelectron spectroscopy analysis showed a reduction in C1s (87.3 to 72.8%) and an increase in O1s (12.7 to 27.2%), indicating cellulose oxidation and chain scission. These results demonstrate that low-density corn-husk plywood combines strong thermal and acoustic performance with inherent photodegradability, making it a promising sustainable building material.

1. Introduction

Petroleum-based door panels, primarily made from acrylonitrile-butadiene-styrene (ABS) polymer, are widely used in modern architecture.(1) These materials offer excellent water resistance, corrosion resistance, and relatively low cost, making them suitable for construction applications. However, their environmental impact remains a primary concern.

Petroleum-based polymers rely on nonrenewable petrochemical resources, generate significant carbon emissions during production, and exhibit poor recyclability at the end of their service life.(2) In the context of global efforts to mitigate climate change and achieve the United

*Corresponding author: e-mail: scshi@ncku.edu.tw
https://doi.org/10.18494/SAM6340

ISSN 0914-4935 © MYU K.K.
https://myukk.org/

Nations' sustainable development goals (SDGs), the increasing demand for eco-friendly, low-carbon, and recyclable alternatives has intensified research on sustainable materials.[3–9]

In recent years, significant attention has been directed toward the development of sustainable insulation materials derived from natural fibers and agricultural waste. These materials have demonstrated promising thermal and acoustic performance while offering advantages such as biodegradability, low environmental impact, and reduced carbon footprint. Recent studies have revealed that natural-fiber-based composites exhibit enhanced insulation properties owing to their inherently porous and hierarchical structures, which facilitate both thermal resistance and acoustic energy dissipation.[10,11]

For example, natural waste biocomposites have been reported to achieve sound absorption coefficients in the range of 0.6–0.8 at mid-to-high frequencies, and even up to 0.9 under optimized porous structures, demonstrating their strong potential as sustainable acoustic materials.[12]

Plywood has emerged as a promising candidate because it requires only a simple hot-pressing process during fabrication, resulting in low energy consumption and cost. Beyond traditional wood sources, plywood can be reinforced with agricultural residues and natural fibers.[13,14] Utilizing agricultural byproducts not only reduces environmental burden but also supports a circular economy by transforming waste into value-added materials.[15–17]

Because of their porous structures, natural fibers have attracted attention for acoustic and thermal insulation applications.[18] The porous architecture enhances sound scattering and energy dissipation, providing great potential for sound absorption. Among various residues, corn husk is particularly attractive because it is one of the most abundant agricultural wastes, cost-effective, and naturally layered, enabling simple lamination for multilayer structures.[19,20]

Cellulose, the primary structural component of corn husk, is a β-1,4-linked glucose polymer.[21–25] However, one challenge for natural fibers is their susceptibility to UV degradation. Under UV irradiation, high-energy photons excite molecules from the ground to unstable excited states, readily forming free or peroxy radicals. These radicals attack β-1,4-glycosidic bonds, cleaving the polymer chain.[26] Progressive chain scission leads to cellulose degradation into smaller molecules and volatile products, reducing material strength and durability.

In this work, the novelty lies not only in the combined evaluation of thermal and acoustic properties, but also in establishing a quantitative structure-property-degradation relationship within a single material system. By systematically varying density and thickness, we reveal how internal porosity simultaneously governs heat transfer, sound dissipation, and susceptibility to photodegradation.

Importantly, the results demonstrate a clear performance trade-off, where increased porosity enhances thermal insulation and acoustic absorption but accelerates light-induced degradation. This integrated approach provides insights that cannot be obtained when these properties are investigated independently.

Such understanding is essential for designing sustainable building materials that require a balance between functional performance and environmental degradability. The ultimate direction of this work is to advance eco-friendly, high-performance construction materials derived from agricultural waste, supporting carbon reduction strategies and circular economy practices.

2. Materials and Methods

2.1 Materials

Corn husk was purchased from a local market. Sodium hydroxide (Panreac AppliChem ITW reagents, Barcelona, Spain), chitosan powder (Charming & Beauty Co., Taipei, Taiwan; Panreac AppliChem ITW reagents, Barcelona, Spain), acetic acid (Charming & Beauty Co., Taipei, Taiwan; Panreac AppliChem ITW reagents, Barcelona, Spain), and glycerol (Katayama Chemical, Japan) were used as received.

2.2 Sample preparation

Raw corn husks were washed with tap water, immersed in 1 M sodium hydroxide solution (DI water:NaOH = 40:1), and stirred on an electromagnetic hotplate at 75 °C for 20 min. After alkaline treatment, the husks were rinsed with tap water, frozen for 24 h, and dried in a vacuum oven for 24 h.

Chitosan powder (7 wt%) and glycerol (7 wt%) were dissolved in DI water and stirred at 75 °C for 20 min. Acetic acid (2 wt%) was then added, and the mixture was stirred for 1 h at 75 °C to obtain the chitosan-based adhesive. Treated corn husks were cut to 100 × 100 mm and coated with 2 g of adhesive. Layers were stacked with perpendicular fiber orientation until the target thickness and density were achieved. Stacks were hot-pressed under the conditions in Table 1 for 0.5 h and cooled in the press for 24 h. Figure 1 shows natural plywood prepared from corn husks, an agricultural byproduct. The husks were stacked perpendicularly and bonded by

Table 1
Relationship between pressure, number of layers, thickness, and density of plywood samples.

Thickness (mm)	Density (kg/m^3)	Pressure (kg)	Number of layers	Sample code
3	1000	500	25	3-1000
3	800	200	20	3-800
3	600	100	15	3-600
5	1000	500	40	5-1000
5	800	200	35	5-800
5	600	100	30	5-600
10	1000	500	90	10-1000
10	800	200	70	10-800
10	600	100	60	10-600

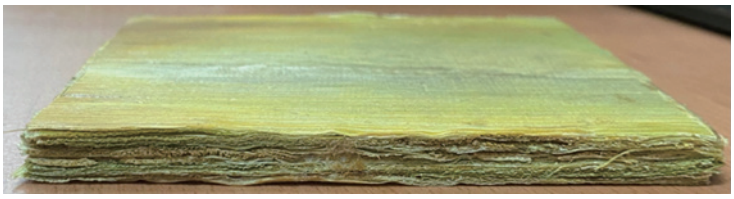


Fig. 1. (Color online) Natural plywood made from stacked corn husks.

hotpressing to form layered plywood. Its intrinsic porosity and fibrous structure cause internal voids and thickness to affect sound absorption and thermal insulation.

2.3 Performance tests

A custom small-scale reverberation chamber was used to measure sound absorption. The reverberation time to 30 dB (RT30) of the empty chamber was first measured using REW software (500–8000 Hz) and converted to RT60_before using Eq. (1). The sample was then placed in the chamber to measure RT30 and calculate RT60_after. The absorption coefficient at each frequency was obtained with Eq. (2) using the difference in reverberation time.

The chamber was designed with a nonsymmetric geometry to reduce standing wave and resonance effects, thereby improving sound field uniformity. Because of the limited chamber size, RT60 values were estimated from the measured RT30 values, and the valid frequency range of the setup was above 500 Hz. Therefore, the results are primarily intended for comparative analysis rather than absolute standardized measurements.

For comparison, a commercial acrylonitrile butadiene styrene (ABS) sheet was included as a reference material representing conventional door panel applications. The ABS samples were prepared with the same thickness as the plywood specimens and evaluated under identical acoustic measurement conditions. This ensured consistency in testing procedures and enabled a direct performance comparison under the same experimental setup.

$$RT60 = RT30 \times 2 \tag{1}$$

$$\alpha = \frac{55.3\ \mathrm{V}}{Sc}\left(\frac{1}{RT60_{after}} - \frac{1}{RT60_{before}}\right) \tag{2}$$

Thermal conductivity and specific heat capacity were measured using a Hot Disk TPS 2500s analyzer, where two specimens (>12 mm) were placed around the sensor with a 20 mW heat input for 20 s.

The temperature was recorded at 5 s intervals for a total duration of 3600 s to evaluate insulation performance. Photodegradation behavior was studied by exposing corn-husk samples

(ASTM D638 type V and 5 × 5 mm^2) to full-spectrum UV-A lamps with a peak at 400 cm^{-1} and visible light at 450–700 cm^{-1} at 30000 Lux from a distance of 10 cm inside a humidity-controlled chamber.

The exposure was carried out for 0, 7, 14, 21, and 28 days, with samples retrieved weekly for analysis. X-ray photoelectron spectroscopy (PHI VersaProbe 4) was used to analyze C1s and O1s signals. Mechanical performance was evaluated using a universal testing machine at 5 N/s.

3. Results and Discussion

3.1 Sound absorption coefficient

Figures 2(a)–2(c) show the sound absorption coefficients of plywood of 3, 5, and 10 mm thicknesses with various densities (600, 800, and 1000 kg/m^3). The coefficients were calculated from the difference in RT60 using Eq. (2), and the curves also include data of reference vinyl from JCW Acoustic Supplies, whose absorption behavior matched the ABS measured in the small reverberation chamber, confirming the reliability of the method. The absorption coefficient increased as density decreased, particularly in the 4000–8000 Hz range; shorter wavelengths enhanced internal reflection and scattering.[27]

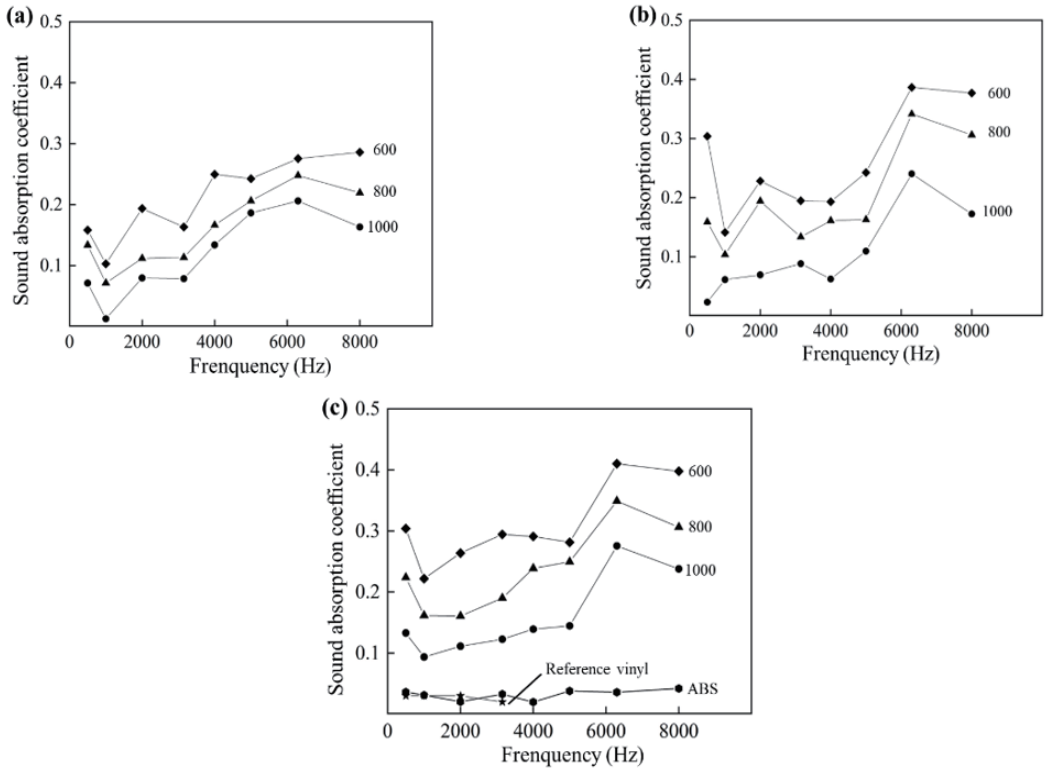


Fig. 2. Sound absorption coefficients of plywood at (a) 3, (b) 5, and (c) 10 mm from 500 to 8000 Hz.

This enhanced performance at higher frequencies is attributed to the shorter sound wavelengths, which become comparable to the characteristic pore size and internal fiber spacing of the plywood, leading to increased multiple scattering and energy dissipation through viscous and thermal losses within the porous structure.[28]

Lower-density samples (600 kg/m³) consistently exhibited better absorption because their internal porosity dissipates sound energy more effectively. Thickness also played a significant role, as thicker boards provided longer paths and more interfaces for wave propagation, increasing acoustic impedance and promoting faster energy decay.

In contrast, sound absorption in the low-frequency region remained limited owing to the longer wavelengths, which are less effectively attenuated by the relatively thin structure (3–10 mm) of the plywood. Additionally, the thickness is insufficient to support resonance or quarter-wavelength absorption mechanisms typically required for efficient low-frequency attenuation. This behavior is consistent with classical porous media models, such as the Johnson-Champoux-Allard framework, which describe frequency-dependent viscous and thermal dissipation in porous materials.[29]

The 10-mm-thick plywood exhibited the highest overall sound absorption coefficient because sound waves traveling through thicker panels encounter more internal interfaces, dissipating acoustic energy more effectively. As a result, the reflected sound energy is weaker and the overall energy attenuation occurs more rapidly. The sound absorption coefficient of sample 10-600 reached 0.410 at 6300 Hz with an average coefficient of 0.308, exceeding the standard criterion of 0.200 for effective sound-absorbing materials.

The relationship between density and porosity in this system can be interpreted in terms of the presence of air-filled voids within the material. A decrease in bulk density corresponds to an increase in the volume fraction of voids (apparent porosity). In this context, density serves as an indirect quantitative indicator of porosity, where lower density indicates higher void content, thereby enhancing both acoustic absorption and thermal insulation performance.

3.2 Thermal conductivity of the plywood

Figure 3(a) shows the relationship between density, thermal conductivity, and specific heat. In contrast, Fig. 3(b) shows thermal resistance versus thickness. Test results indicated that thermal conductivity and specific heat increased with density because denser structures reduced internal void content and enhanced solid-to-solid heat conduction.

Specific heat increased with density, meaning the material stored more thermal energy and showed improved thermal stability. Thermal resistance increased with thickness because heat traveled a longer path through more material interfaces, raising the energy flow barrier. Low-density plywood showed higher thermal resistance at the same thickness because its porous structure interrupted heat transfer.

For comparison, 10 mm-thick ABS exhibited a thermal conductivity of approximately 0.22 W/(m·K) and a thermal resistance of 0.045 m²·K/W,[30] both of which fell between the corresponding values of plywood samples 10-1000 and 10-800.

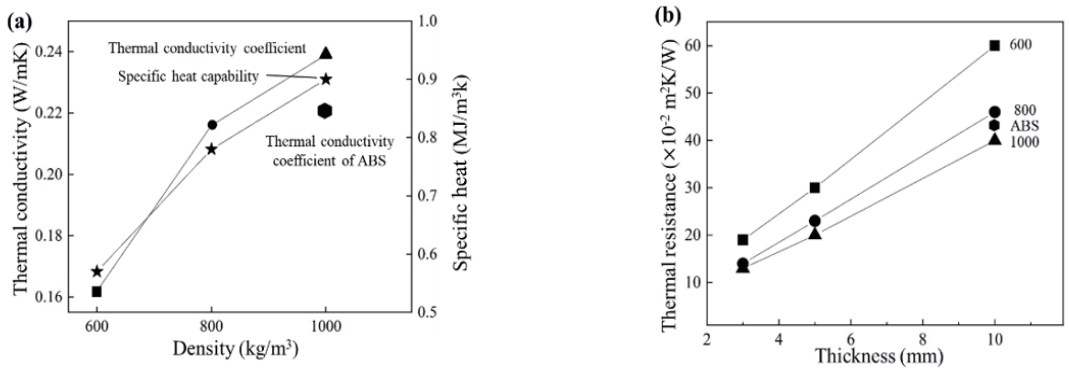


Fig. 3. (a) Thermal conductivity and specific heat versus density. (b) Thermal resistance versus thickness for plywood and ABS.

Thermal insulation performance in this system is governed by both thermal conductivity and volumetric heat capacity ($\rho \cdot c_p$). Thermal conductivity controls the rate of heat transfer under steady-state conditions, where lower k results in better insulation. In contrast, the volumetric heat capacity determines the ability of the material to store thermal energy and affects transient heat transfer behavior.

As density increases, both thermal conductivity and $\rho \cdot c_p$ increase. A higher thermal conductivity promotes heat conduction and reduces insulation efficiency under steady-state conditions, whereas a higher $\rho \cdot c_p$ enhances thermal inertia by delaying heat propagation.[31] Therefore, lower-density samples provide better insulation under steady-state conditions owing to reduced thermal conductivity, while higher-density samples exhibit greater heat storage capacity under transient conditions.

3.3 Mechanical properties and weight loss ratio

The mechanical integrity of corn-husk plywood is strongly affected by the effectiveness of interfacial bonding between adjacent layers. In this study, the chitosan-based adhesive plays a key role in enhancing this bonding. Because of the presence of amino ($–NH_2$) and hydroxy (–OH) functional groups, chitosan undergoes hydrogen bonding interactions with cellulose fibers, which improves interfacial adhesion and facilitates stress transfer across layers.[32,33]

Furthermore, during hot pressing, the adhesive softens and partially penetrates into the porous structure of the corn husk, leading to enhanced mechanical interlocking and fewer interfacial voids.[34] This contributes to a more uniform stress distribution under tensile loading. The presence of glycerol as a plasticizer also increases the flexibility of the adhesive phase, reducing interfacial brittleness and delaying crack initiation.

Table 2 and Fig. 4 show the full-range X-ray photoelectron spectroscopy (XPS) spectra and quantitative results for corn-husk surfaces before irradiation and after 28 days of light exposure. The intensity of the C1s peak at 285.70 eV decreased from 87.3 to 72.8%, while that of the O1s

Table 2
XPS quantitative analysis results of C and O at days 0 (D0) and 28 (D28).

Region	Parameter	D0	D28
C1s	Content (%)	87.30	72.80
	Binding energy (eV)	285.70	
	Intensity (arb. unit)	38368.75	29893.75
O1s	Content (%)	12.70	27.20
	Binding energy (eV)	564.08	
	Intensity (arb. unit)	11750.00	16762.50

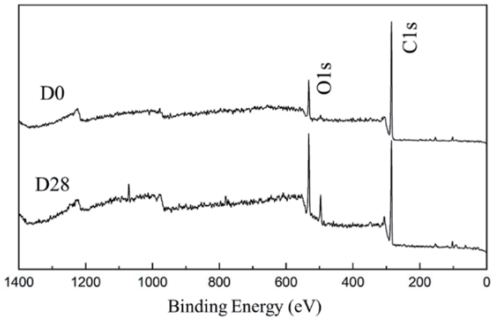


Fig. 4. XPS spectra of corn husk at days 0 and 28.

peak at 564.08 eV increased from 12.7 to 27.2%. Peak intensity changes were consistent with surface chemical modification during the photodegradation test.

During light exposure, oxidation generates free radicals and reactive oxygen species that attack β-1,4-glycosidic bonds in cellulose. This mechanism breaks the cellulose backbone, forms oxygen-containing functional groups, and volatilizes or oxidizes carbon chains. Consequently, the intensity of the O1s peak rises while that of the C1s peak declines.[35] These chemical changes indicate the progressive degradation of the cellulose network, which weakens intermolecular interactions and disrupts structural continuity. The resulting reduction in molecular integrity promotes the formation of microstructural defects and decreases the efficiency of load transfer within the material.

The XPS results confirm that prolonged light exposure promotes surface oxidation and functional group transformation. Increased oxygen content indicates the enhanced photodegradation susceptibility of corn-husk plywood surfaces. This behavior matches the degradation pathway proposed in the introduction.

Figure 5 shows the tensile behavior and weight loss ratio of corn-husk materials after various UV exposure times. Figure 5(a) presents the trend of tensile strength versus the number of irradiation days, and Fig. 5(b) shows engineering stress-strain curves. Tensile strength gradually decreased with prolonged exposure, and the D0 sample exhibited the highest stress limit, while the D28 sample showed the lowest tensile capacity and ductility.

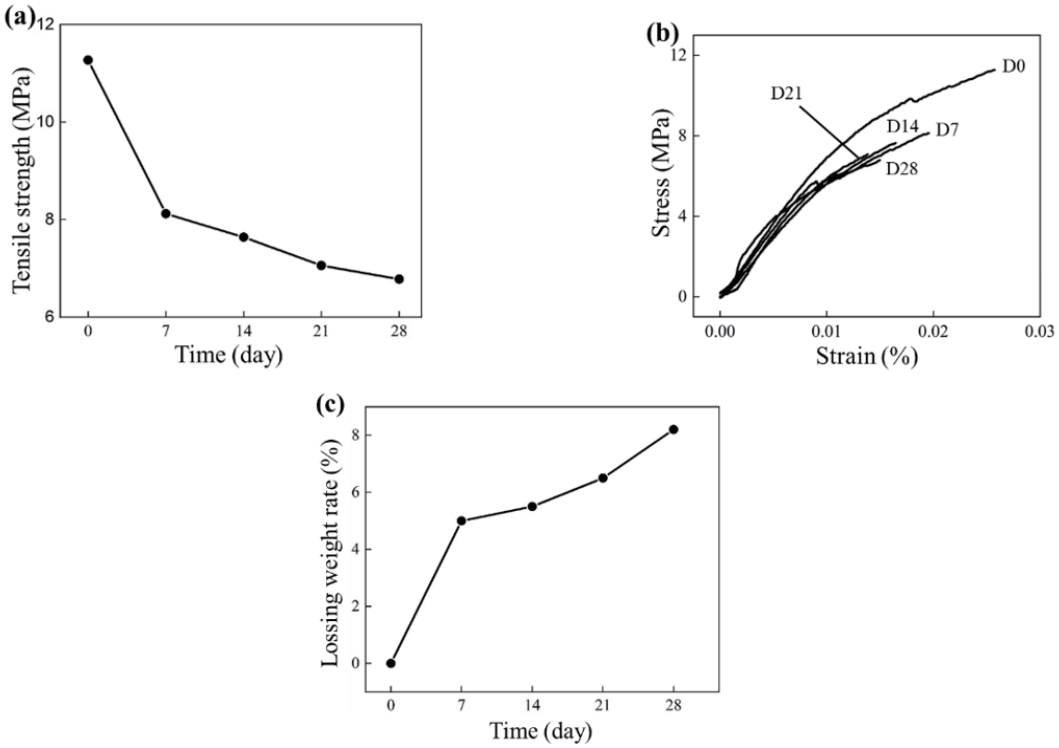


Fig. 5. (a) Tensile strength vs UV exposure time, (b) engineering stress-strain curves, and (c) weight loss ratio vs UV exposure time.

These behaviors are consistent with those in previous studies. For example, in regenerated cellulose-fiber-reinforced polyamide systems, UV exposure has been reported to induce a more pronounced reduction in tensile strength, particularly at elevated temperatures, indicating synergistic degradation effects.[36]

This degradation is attributed to the generation of free radicals upon UV light irradiation, which cleave C–C and C–O bonds in cellulose. The bond cleavage produces small gaseous molecules such as CO, CO_2, and CH_4,[37] resulting in partial mass loss. Concurrently, the crystalline regions of cellulose break down, reducing crystallinity and producing a looser structure. Figure 5 also displays the fracture surfaces of samples after 0, 7, 14, and 21 days of irradiation. The D0 sample fractured at a single, concentrated site, while longer exposures produced more dispersed and ragged breaks. By 21 and 28 days, torn edges and fiber bundle detachment were evident, indicating reduced toughness and structural uniformity.

The observed mechanical degradation is closely related to the underlying microstructural evolution during UV exposure. XPS results reveal increased oxidation and the formation of oxygen-containing functional groups, indicating chain scission in the cellulose structure. This chemical degradation weakens the integrity of the fiber network and reduces the effectiveness of load transfer across fibers. In addition, the formation of microstructural defects and increased heterogeneity promote stress concentration, facilitating crack initiation and propagation.

This behavior is consistent with the observed fracture morphology, where the D0 sample exhibits a more localized fracture, while prolonged UV exposure results in more dispersed and irregular fracture patterns. Consequently, the combined effects of chain scission, structural weakening, and defect formation lead to the observed decreases in tensile strength and ductility.

Although the results of the present study demonstrate promising thermal and acoustic performance, several limitations should be considered to enable real-world applications. Natural-fiber-based materials are inherently sensitive to environmental factors such as UV radiation, moisture, and temperature variations, which may lead to long-term degradation. The XPS and mechanical results in this study indicate that UV exposure promotes oxidation and chain scission, which can gradually degrade structural integrity and mechanical performance.

In addition, moisture absorption may further affect dimensional stability and durability. Therefore, improving long-term stability remains a key challenge. Future work should include the exploration of strategies such as surface coatings, chemical modification, or hybrid composite design to enhance environmental resistance while maintaining sustainability.

4. Conclusions

In this study, we fabricated plywood of various densities and thicknesses using different hot-pressing pressures. Experimental results showed that lower density increased internal porosity, which enhanced energy dissipation through multiple medium interfaces. Thicker plywood further improved energy attenuation, confirming the critical roles of porosity and thickness in thermal and acoustic performance.

Thermal and acoustic analyses demonstrated that low-density plywood exhibits superior sound absorption compared with ABS. Sample 10-600 achieved a thermal conductivity of 0.162 W/m·K and a heat capacity of 0.57 MJ/m^3·K, both of which are lower than those of ABS.

The photodegradation behavior of corn-husk plywood was also evaluated under 28 days of visible and UV-A exposure. XPS analysis showed that the C1s peak intensity decreased by 14.5% and that of the O1s peak increased by 14.5%, while tensile strength dropped by 60% and weight loss reached 8.2%. These findings confirm that the material exhibits effective light-driven degradability. Future work will focus on enhancing durability while maintaining eco-friendly thermal and acoustic properties for sustainable building applications.

Acknowledgments

This work was supported by the National Science and Technology Council (NSTC), Taiwan (Grant Nos. 113-2221-E-006-087-MY2, 113-2221-E-006-112-MY2, 114-2221-E-006-090, 115-2221-E-006-114, 115-2221-E-006-066-MY2, and 115-2622-E-006-017). The authors acknowledge the Core Facility Center of National Cheng Kung University, Taiwan, for access to SEM3202. Additional support from the Higher Education Sprout Project, Ministry of Education, Taiwan, through the Headquarters of University Advancement at National Cheng Kung University (NCKU), is also gratefully acknowledged.

References

1 S. Olivera, H. B. Muralidhara, K. Venkatesh, K. Gopalakrishna, and C. S. Vivek: J. Mater. Sci. **51** (2016) 3657. https://doi.org/10.1007/s10853-015-9668-7
2 S. Rajendran, A. Al-Samydai, G. Palani, H. Trilaksana, T. Sathish, J. Giri, R. Saravanan, J. I. J. Lalvani, and F. Nasri: Eng. Rep. **7** (2025) e70108. https://doi.org/10.1002/eng2.70108
3 D. Rahmadiawan, N. Aslfattahi, N. Nasruddin, R. Saidur, A. Arifutzzaman, and H. A. Mohammed: J. Nano Res. **68** (2021) 17. https://doi.org/10.4028/www.scientific.net/JNanoR.68.17
4 D. Rahmadiawan, S. C. Shi, Z. Fuadi, H. Abral, N. Putra, R. Irwansyah, D. Gasni, and A. M. Fathoni: J. Tribol. **39** (2023) 36.
5 D. Rahmadiawan, S. C. Shi, N. Aslfattahi, A. N. Fauza, and Z. Fuadi: ACS Omega **10** (2025) 36878. https://doi.org/10.1021/acsomega.5c05037
6 A. Martin, E. Taer, N. Nasruddin, and N. Khotimah: Teknomekanik **8** (2025) 52. https://doi.org/10.24036/teknomekanik.v8i1.36172
7 H. Nurdin, W. Waskito, D. Harmanto, P. Purwantono, A. Kurniawan, D. Yuvenda, and Y. M. Anaperta: Teknomekanik **8** (2025) 24. https://doi.org/10.24036/teknomekanik.v8i1.33672
8 S.-C. Shi, T.-F. Huang, and J.-Y. Wu: Materials **8** (2015) 1738. https://doi.org/10.3390/ma8041738
9 Kadriadi, D. Rahmadiawan, H. Abral, Ilhamdi, M. Ivan, Akmal, D. Handayani, L. R. Septria Ningrum, R. S. Masri, B. A. Widyaningrum, M. H. Mohamad Kassim, and M. Mahardika: Food Biosci. **68** (2025) 106500. https://doi.org/10.1016/j.fbio.2025.106500
10 R. Ahmed, K. H. Manik, A. Nath, J. R. Shohag, J. J. Mim, and N. Hossain: Mater. Today Sustainability **32** (2025) 101220. https://doi.org/10.1016/j.mtsust.2025.101220
11 M. Ouda, A. A. Abu Sanad, A. Abdelaal, A. Krishna, M. Kandah, and J. Kurdi: Buildings **15** (2025) 2876. https:/doi.org/10.3390/buildings15162876
12 M. Namakka, M. R. Rahman, M. K. B. Bakri, B. D. Karuppasamy, M. S. Ahmmad, A. A. James, and I. M. M. Rahman: Adv. Compos. Hybrid Mater. **8** (2025) 386. https://doi.org/10.1007/s42114-025-01427-6
13 Z. Wang, S. Zhao, H. Kang, W. Zhang, J. Li, S. Zhang, and A. Huang: J. Cleaner Prod. **210** (2019) 1366. https://doi.org/10.1016/j.jclepro.2018.10.326
14 R. A. Nabawi, S. Syahril, and H. Abral: Teknomekanik **8** (2025) 243. https://doi.org/10.24036/teknomekanik.v8i2.52472
15 Y.-T. Chen, S.-C. Shi, and D. Rahmadiawan: Sens. Mater. **37** (2025). http://doi.org/10.18494/sam5447
16 M. I. Ammarullah, I. Y. Afif, M. I. Maula, T. I. Winarni, M. Tauviqirrahman, and J. Jamari: Mate. Today: Proc. **63** (2022) S143. https://doi.org/10.1016/j.matpr.2022.02.055
17 I. Sopiyan, T. P. Soemardi, H. Purnomo, and O. Polit: Teknomekanik **8** (2025) 117. https://doi.org/10.24036/teknomekanik.v8i1.36572
18 T. Yang, L. Hu, X. Xiong, M. Petrů, M. T. Noman, R. Mishra, and J. Militký: Sustainability **12** (2020) 8477. https://doi.org/10.3390/su12208477
19 X. Tang, X. Zhang, H. Zhang, X. Zhuang, and X. Yan: Appl. Acoust. **134** (2018) 60. https://doi.org/10.1016/j.apacoust.2018.01.012
20 F.-M. Lin, P.-Y. Hong, and C.-Y. Lee: Appl. Acoust. **71** (2010) 68. https://doi.org/10.1016/j.apacoust.2009.06.005
21 S.-C. Shi, T.-H. Chen, and P. K. Mandal: Polymers **12** (2020) 1246. https://doi.org/10.3390/polym12061246
22 S. Keerthiveettil Ramakrishnan, K. Vijayananth, A. Arivendan, and M. I. Ammarullah: Results Eng. **24** (2024) 102974. https://doi.org/10.1016/j.rineng.2024.102974
23 S. Keerthiveettil Ramakrishnan, K. Vijayananth, A. Arivendan, and M. I. Ammarullah: Sci. Rep. **15** (2025) 4611. https://doi.org/10.1038/s41598-025-88058-5
24 S.-C. Shi, X.-N. Tsai, and D. Rahmadiawan: Surf. Coat. Technol. **483** (2024) 130712. https://doi.org/10.1016/j.surfcoat.2024.130712
25 A. Amri, D. E. Putri, D. Febryza, S. D. Voadi, S. P. Utami, H. A. Miran, and M. M. Rahman: Teknomekanik **7** (2024) 139. https://doi.org/10.24036/teknomekanik.v7i2.32972
26 P. Saha, S. Manna, D. Roy, M. C. Kim, S. Chowdhury, S. De, R. Sen, B. Adhikari, and J. K. Kim: Fibers Polym. **15** (2014) 2345. https://doi.org/10.1007/s12221-014-2345-7
27 S. Kuznetsova, S. Deleplanque, F. Allein, B. Dubus, and M. Miniaci: Proc. R. Soc. A **480** (2024) 20230831. https://doi.org/10.1098/rspa.2023.0831
28 X. Cai, J. Yang, G. Hu, and T. Lu: J. Acoust. Soc. Am. **144** (2018) EL138. httsp://doi.org/10.1121/1.5051526
29 S. Kuznetsova, F. Allein, V. F. Dal Poggetto, F. X. Bécot, and M. Miniaci: npj Acoust. **1** (2025) 25. https://doi.org/10.1038/s44384-025-00023-8
30 A. Rodriguez, J. P. Fuertes, A. Oval, and G. Perez-Artieda: Materials **16** (2023) 7384. https://doi.org/10.3390/ma16237384

31 F. Collet and S. Pretot: Constr. Build. Mate. **65** (2014) 612. https://doi.org/10.1016/j.conbuildmat.2014.05.039
32 L. Kumar, S. C. Agwuncha, P. Tyagi, and L. Pal: Food Packag. Shelf Life **52** (2025) 101613. https://doi.org/10.1016/j.fpsl.2025.101613
33 L. Dai, Y. Geng, X. Ding, Z. Zhang, C. Lai, D. Zhang, C. Xia, and Y. Lai: Carbohydr. Polym. **366** (2025) 123869. https://doi.org/10.1016/j.carbpol.2025.123869
34 F. Fodor and M. Bak: Materials **16** (2023) 2046. https://doi.org/10.3390/ma16052046
35 X.-Q. Wang, H.-Q. Ren, R.-J. Zhao, Q. Cheng, and Y.-P. Chen: Spectrosc. Spectral Anal. **29** (2009) 1864. https://doi.org/10.3964/j.issn.1000-0593(2009)07-1864-04
36 C. K. Falkenreck, J.-C. Zarges, and H.-P. Heim: Sci. Rep. **16** (2026) 13770. https://doi.org/10.1038/s41598-026-51172-z
37 L. Brandt, C. Bohnet, and J. King: J. Geophys. Res.: Biogeosci. **114** (2009). https://doi.org/10.1029/2008JG000772